

Article

# Photodegradation of Polycyclic Aromatic Hydrocarbons from Coal Tar into Mine Wastewaters and Sewage Wastewater on a Flat-Bed Photoreactor

Jean Bedel Batchamen Mougno<sup>1,\*</sup> , Frans Waanders<sup>1</sup> , Elvis Fosso-Kankeu<sup>2</sup>  and Ali R. Al Alili<sup>3</sup>

<sup>1</sup> Water Pollution Monitoring and Remediation Initiatives Research Group, Centre of Excellence in Carbon-Based Fuels, North-West University, Private Bag X6001, Potchefstroom 2520, South Africa; frans.waanders@nwu.ac.za

<sup>2</sup> Department of Mining Engineering, College of Science Engineering and Technology, University of South Africa, Florida Science Campus, Johannesburg 2028, South Africa; elvisfosso.ef@gmail.com

<sup>3</sup> DEWA R&D Centre, Dubai Electricity and Water Authority (DEWA), Dubai P.O. Box 564, United Arab Emirates; ali.alalili@ku.ac.ae

\* Correspondence: 37465597@student.g.nwu.ac; Tel.: +27-78-123-3917

**Abstract:** Wastewater treatment has been widely focused on the undesirable pollutants derived from various activities such as coking, coal gasification, oil spills, and petroleum. These activities tend to release organic pollutants, however polycyclic aromatic hydrocarbons (PAHs) happen to be highlighted as the most carcinogenic pollutant that easily comes into contact with the environment and humans. It causes major challenges due to its lingering in the environment and chemical properties. Although various techniques such as ions exchange, advanced oxidation, and reverse osmosis have been conducted, some of them have been ignored due to their cost-effectiveness and ability to produce a by-product. Therefore, there is a need to develop and implement an effective technique that will alleviate the organic pollutants (PAHs) in various water sources. In this study, a self-made flat-bed photoreactor was introduced to degrade PAHs in various water sources such as acidic mine drainage, alkaline mine drainage, and sewage wastewater. A previous study was conducted, and only 7.074 mg/L, 0.3152 mg/L and 1.069 mg/L in 4 weeks and thereafter 19.255 mg/L, 1.615 mg/L and 1.813 mg/L in 8 weeks in acidic mine drainage, alkaline mine drainage, and sewage wastewater leachate from a 2916.47 mg/L of PAHs in coal tar, was analysed. It was found that the flat-bed photoreactor was highly effective and able to obtain a removal efficiency of 64%, 55%, and 58%, respectively; without the flat-bed photoreactor, happened the removal efficiency was of 53%, 33%, and 39%, respectively, in 60 min in acidic mine drainage, alkaline mine drainage, and sewage wastewater. The photodegradation of PAHs was favoured in the acidic mine drainage, followed by sewage wastewater and alkaline mine drainage respective, showing time and solar irradiation dependence.

**Keywords:** photoreactor; polycyclic aromatic hydrocarbons; solar irradiation



**Citation:** Batchamen Mougno<sup>1</sup>, J.B.; Waanders, F.; Fosso-Kankeu, E.; Al Alili, A.R. Photodegradation of Polycyclic Aromatic Hydrocarbons from Coal Tar into Mine Wastewaters and Sewage Wastewater on a Flat-Bed Photoreactor. *Pollutants* **2022**, *2*, 333–346. <https://doi.org/10.3390/pollutants2030023>

Academic Editor: Saddam Hussain

Received: 8 June 2022

Accepted: 14 July 2022

Published: 27 July 2022

**Publisher's Note:** MDPI stays neutral with regard to jurisdictional claims in published maps and institutional affiliations.



**Copyright:** © 2022 by the authors. Licensee MDPI, Basel, Switzerland. This article is an open access article distributed under the terms and conditions of the Creative Commons Attribution (CC BY) license (<https://creativecommons.org/licenses/by/4.0/>).

## 1. Introduction

Wastewater treatment is a well-studied topic concerning the release of organic matter (dyes, pharmaceuticals, etc.) and suspended solids (salts, metals, etc.) [1–3]. This wastewater is mostly derived from water pollution that is obtained from various activities such as mining, oil spills, agriculture, burning of coal, etc. These activities happen to release major pollutants, however, most developing countries are responsible for releasing large amounts of pollutants from their extensive production [4]. The petroleum industry is one of the contributors to the release of organic pollutants during energy production through gasification and coking [5], and it is also used to manufacture various products [6]. Coal tar is a by-product of coal that can be formed from fractionation or coking and has polycyclic aromatic hydrocarbons (PAHs) that are predominant and harmful when found in water

sources [7]. The PAHs are known as persistent organic pollutants (POPs) that can be distinguished by their solubility, vapor pressure, and high boiling and melting point [1].

It is important to identify their molecular weight when considering the removal of the pollutant, and their increase in molecular weight contributes to the oxidation and reduction [8]. The maturity of the crude oil or coal tar supposedly increases the molecular weight of PAHs over time [9]. Anthropogenic activities such as oil seeps, volcanic eruptions, human activities, crude oil, coal tar, and petroleum spills can also contribute to the release of PAHs in the environment [5]. The stability of the PAHs in the environment can be described by their molecular weight and structures [5]. It was reported by Cai et al. [10] that a lower number of molecular rings of 2 and 3 of PAHs mean that they have greater solubility in water and easily undergo destabilization and degradation as compared to the heavy molecular rings of 4 rings and above. The PAHs mostly consist of carbon and hydrogen, and their structure can be configured in a linear, angular, or cluster formation [10]. It was discovered by Batchamen Mougnolet et al. [11] that the leaching of PAHs is quick in the acidic mine drainage as compared to the alkaline mine and sewage wastewater, which was caused by pH and the total dissolved organic carbon in the water sources.

There are more than 100 PAHs that are derived from various activities, however, only 16 PAHs have been recognized by the United State Environmental Protection Agency (U.S. EPA, Washington, DC, USA) and European to be human carcinogens and also widely present in various water sources [12]. The 16 PAHs, as presented in Table 1, have been discussed in various studies with regard to their molecular weight and toxicity level [13]. It has been reported by Smol et al. [14] that the PAHs with a lower molecular weight (LMW) undergo a faster degradation as compared to those with a heavy molecular weight (HMW). Moreover, the solubility of PAHs is dependent on their molecular weight [14]. Table 1 represents the characteristics of the 16 PAHs that are found in the environment and various water sources based on the U.S. EPA.

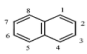
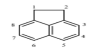
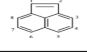
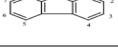
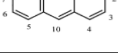
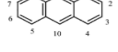
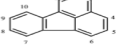
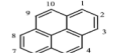
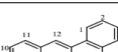
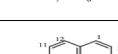
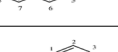
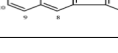
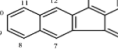
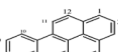
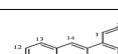
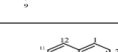
The potential health-related issue resulting from the excessive consumption of PAHs such as skin irritation, inflammation, immune dysfunction, and damage to both kidneys and liver have made them unwanted and unfriendly to the environment. These PAHs also lead to the biological destruction of human cells due to their carcinogenic and mutagenic properties [5,15,16]. Because of their adverse effects, it has been prioritized as the pollutant that is in contact with humans the most, according to the U.S. Environmental Protection Agency (USEPA) [16–19].

The release of these PAHs can also homogeneously change the physio-chemistry of the sewage wastewater, alkaline mine drainage, acid mine drainage, and possible other water sources. Sewage wastewater contains various other pollutants that have been studied in conversion to energy [20]. Most organics such lipids, fats, oils, and heterogeneous and inorganic materials are mostly found in sewage wastewater [21]. The viscosity of sewage wastewater is due to its hydrophobic property [22]. Some metals, such as arsenic (As), cadmium (Cd), chromium (Cr), copper (Cu), mercury (Hg), manganese (Mn), nickel (Ni), lead (Pb), and Zinc (Zn) have similar carcinogenic and mutagenic properties as PAHs [23]. Sewage properties can allow for the adsorption of suspended particles that represent a threat to ecosystems [24]. Various parameters such as total dissolved solids (TSD), pH, temperature, nitrate, nitrite, phosphate, chloride, biologic oxygen demand (BOD), sulphate, ammonium ion, chemical oxygen demand (COD), and alkalinity [25,26]. The deposition of PAHs in acidic mine drainage, alkaline mine drainage, and sewage wastewater has not received attention [11].

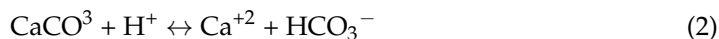
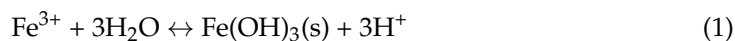
Acidic mine drainage has been widely noted to be the world's largest problem, and this has been revealed by various studies [27]. The term AMD has been recently used instead of acidic rock drainage (ARD) and sulphide oxidation, which was previously used [28]. AMD is formed in a process that occurs in most mining activities due to sulphide reactions, often in the presence of microorganisms, temperature, water, and oxygen in a mine region through a geology function. These mechanisms are variable for different mine regions [29]. The destruction of the mineralized material also leads to AMD and is detrimental to the

environment and humans by damaging various agro species such as plants, fauna, and water, leading to a major cost. AMD is a strong acidic wastewater that contains both ferrous and non-ferrous materials, as well as salts. Among the ferrous materials, there are also some other toxic metals such as As, Cd, Cr, Cu, Zn, Ca, Mg, Al, Mn, Ni, and Pb that contribute to the acidic mine drainage; these are found in small concentrations in the ppm range [29–31]. The alkalinity can be generated through a process of sulphate reduction and carbonate dissolution. On the other hand, a sufficient concentration of carbonate ( $\text{CaCO}_3$ ), bicarbonate ( $\text{HCO}_3^-$ ), and silicate minerals, can change wastewater to be alkaline [32,33].

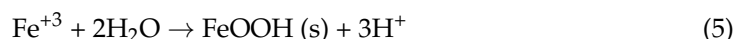
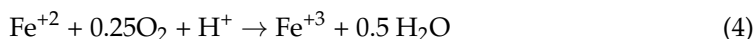
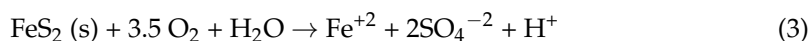
**Table 1.** The 16 PAHs that are commonly found in various water sources [13]. Copyright 2020, copyright owner's A.O. Adeniji.

PAHs	Chemical Formula	Molecular Weight (g/mol)	Rings Number	Melting Point (°C)	Boiling Point (°C)	Structures
Naphthalene (NAP)	$\text{C}_{10}\text{H}_8$	128	2	80.2	218	
Acenaphthylene (ACY)	$\text{C}_{12}\text{H}_8$	152	3	92.5	280	
Acenaphthene (ACE)	$\text{C}_{12}\text{H}_{10}$	152	3	93.4	279	
Fluorene (FL)	$\text{C}_{13}\text{H}_{10}$	166	3	115	295	
Phenanthrene (PHE)	$\text{C}_{14}\text{H}_{10}$	178	3	99.2	340	
Anthracene (ANT)	$\text{C}_{14}\text{H}_{10}$	178	4	215	340	
Fluoranthene (FLU)	$\text{C}_{16}\text{H}_{10}$	202	4	108	384	
Pyrene (PYR)	$\text{C}_{16}\text{H}_{10}$	202	4	151	404	
Benzo[a]anthracene (BaA)	$\text{C}_{18}\text{H}_{12}$	228	4	167	435	
Chrysene (CHY)	$\text{C}_{18}\text{H}_{12}$	228	4	258	448	
Benzo[b]fluoranthene (BbF)	$\text{C}_{20}\text{H}_{12}$	252	5	168	481	
Benzo[k]fluoranthene (Blkf)	$\text{C}_{20}\text{H}_{12}$	252	5	217	480	
Benzo[a]pyrene (BaP)	$\text{C}_{20}\text{H}_{12}$	252	5	177	495	
Dibenzo[a,h]anthracene (DahA)	$\text{C}_{22}\text{H}_{14}$	278	5	270	524	
Indenol [1,2,3-cd] pyrene (IP)	$\text{C}_{22}\text{H}_{12}$	276	6	164	536	
Benzo[g,h,i]perylene (Bghip)	$\text{C}_{22}\text{H}_{12}$	276	6	278	550	

The measure of pH can be used to determine the acidity and alkalinity of the wastewater, and it is in the range of pH 2–8 [32]. The acidic and alkaline reactions are presented in Equations (1) and (2)



AMD is formed by reduced sulphur oxidization in the presence of oxygen and water during destruction [33], and the formation of AMD can be represented in Equations (3)–(5)



Presently, there are still major industries and activities that release PAHs, and according to Rodríguez-Galán, et al. [30], special treatment should be implemented to either treat or monitor the deposition of compounds or by-products that contain PAHs, like the coal pollution in the environment, which cause problems and result in a lot of necessary maintenance and high costs to reduce or treat the pollution.

The increase in the number of rings increases the molecular weight of PAHs and their hydrophobic nature [10]; this has been suggested as an effective method to remove these organic pollutants from living things [34,35]. There are methods such as biological, physical (filtration, precipitation, flocculation, reverse osmosis methods, and adsorption) and chemical (advanced oxidation, ion exchange, coagulation, advanced oxidation, and ozonation) approaches [36] that have been conducted to assist in degrading these PAHs from various water sources [7,37]. There are disadvantages to these, such as the maintenance cost and the release of a toxic by-product when using physical and chemical methods. However, it was pointed out that the biological method is a better candidate to approximately remove 92% of PAHs that are mostly in soil [38,39].

Sunlight is composed of three components that provide a range of wavelengths, namely visible light (400–700 nm), UVA light (320–400 nm), and UVB (280–320 nm), which can be used to degrade PAHs in water sources [40]. The degradation of PAHs can best be monitored using visible light and UVA [40]. The application of the light source can be accommodated with a photoreactor. A photoreactor is a device that is mostly composed of elements that are designed with a specific dimension and geometry to be used for various applications, but this study is aimed at the photodegradation of PAHs. The photoreactor can either be designed with a single channel (the fluid is flowing in one direction) or multiple channels (the fluid is flowing in various directions) [41]. Various photoreactors, such as photocatalytic reactors, have been used for the degradation of organic pollutants. These reactors have been designed to accommodate a catalyst and light source. In this conventional photocatalytic reactor, an additional solar convertor, timer, recycler, cooler or heater exchange, etc, can be mounted to enhance its effectiveness [42,43].

Some photoreactors have advantages and disadvantages in converting energy from solar irradiation to photons [44]. The use of collectors is important in case the photoreactor is unable to provide enough of the necessary energy/photons [45]. However, it all depends on the range of operating temperatures and the efficiency. Collectors such as the flat plate, parabolic mix, evacuated tank, parabolic trough, Fresnel prism, parabolic dish, and heliostat field collectors can be used to enhance the photoreactor effectiveness. The advantages of these collectors, when combining them with optical, thermal and thermodynamic devices, can enhance their performance [46]. A study conducted by Matamoros et al. [47] illustrated that the nature of the environment drastically influences the removal efficiency of pollutants. It was observed that during a warm season, a higher temperature resulted in a higher removal efficiency as compared to a cold season. It was proven that the longer the reaction between the photon and the pollutants, the higher the photodegradation of the pollutants (PAHs) [48].

In this study, the aims are to investigate the effectiveness of a self-made photoreactor on the photodegradation of PAHs in acidic mine drainage, alkaline mine drainage, and sewage wastewater, assisted by solar irradiation. The purpose of this work is to introduce an effective material that is hazardless and cost-effective for the photodegradation of PAHs. Therefore, to achieve this, it is important to improve the effectiveness of solar irradiation by implementing a material that will enhance viability.

## 2. Materials and Methods

In this study, three water sources, namely acidic mine drainage, alkaline mine drainage, and sewage wastewater, were collected at the Witbank (25.8728° S, 29.2553° E), Middleburg (25.7699° S, 29.4639° E) and Cape Town Municipality (33.9249° S, 18.4241° E) in South Africa. The coal tar was obtained at New Castle KwaZulu-Natal (27.7138° S, 29.9972° E), South Africa (30.5595° S, 22.9375° E). These water sources were analysed as previously reported by Batchamen et al. [11].

### 2.1. Degradation Experiments

A 5 g mass of coal tar was added in each water sample, i.e., acidic mine drainage, alkaline mine drainage, and sewage wastewater, for the leaching process [11]. A concentration of 2916.47 mg/L of PAHs in coal was identified using the Gas Chromatography Thermo Scientific (TSQ 8000) apparatus (Cape Town, South Africa) using a Triple Quadrupole MS technique.

The leaching process of the PAHs was conducted, and it was found that 19.255 mg/L, 1.615 mg/L, and 1.813 mg/L of PAHs out of 2916.47 mg/L were dissolved in the acidic mine drainage, alkaline mine drainage, and sewage wastewater, respectively, in 8 weeks. A volume of 300 mL of each of these water sources was used for the photodegradation of the PAHs under solar irradiation respective to time with or without the flat-bed photoreactor. Without the flat-bed photoreactor, 250 mL volume solution was stirred with a magnetic stirrer operated at 250 rates per minute (RPM), as illustrated in Figure 1. A similar procedure was also conducted but this time, with the flat-bed photoreactor being used.

The water samples were collected at each interval of 20 min, 40 min, and 60 min using a 0.45 µm syringe filtered PDVP after the photodegradation. The GC-MS was used to determine the remaining PAHs in each of the water sources so as to investigate the degraded PAHs, and the results are presented in Tables 3 and 4. The degraded PAHs were calculated using Equation (6) and the removal efficiency using Equation (7).

$$\text{PAHs}_{\text{initial}} - \text{PAHs}_{\text{final}} = \text{PAHs}_{\text{degraded}} \quad (6)$$

$$\text{PAHs removal efficiency (RE) (\%)} = \frac{C_o - C_t}{C_o} \times 100\% \quad (7)$$

where  $C_o$  is the initial concentration of PAHs and  $C_t$  is the concentration after the photodegradation respective to time ( $t$ ).

A similar experiment was conducted but this time with a flat-bed photoreactor. The flat-bed photoreactor was made of Perspex material (AXSC0230502050I) and used for the study. Their dimension unit is given in millimetres (mm) (Figure 2). The box was used to maintain the photon energy within the system.

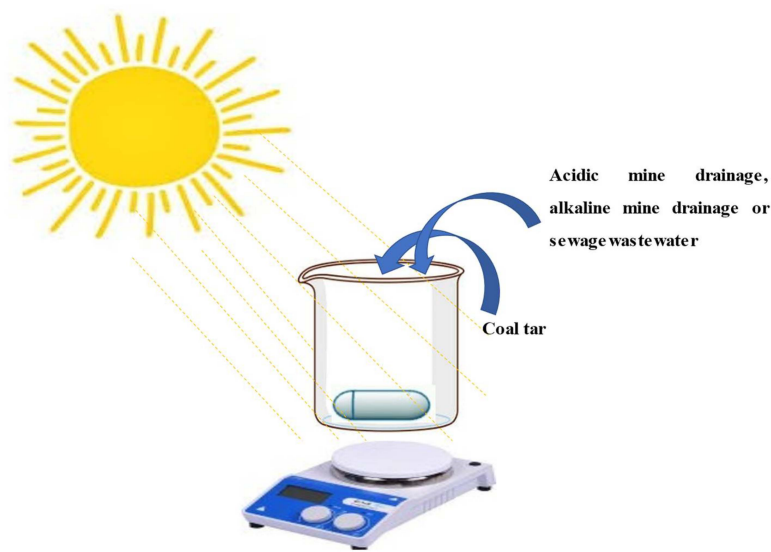


Figure 1. Experimental setup for the photodegradation of PAHs without a flat-bed photoreactor.

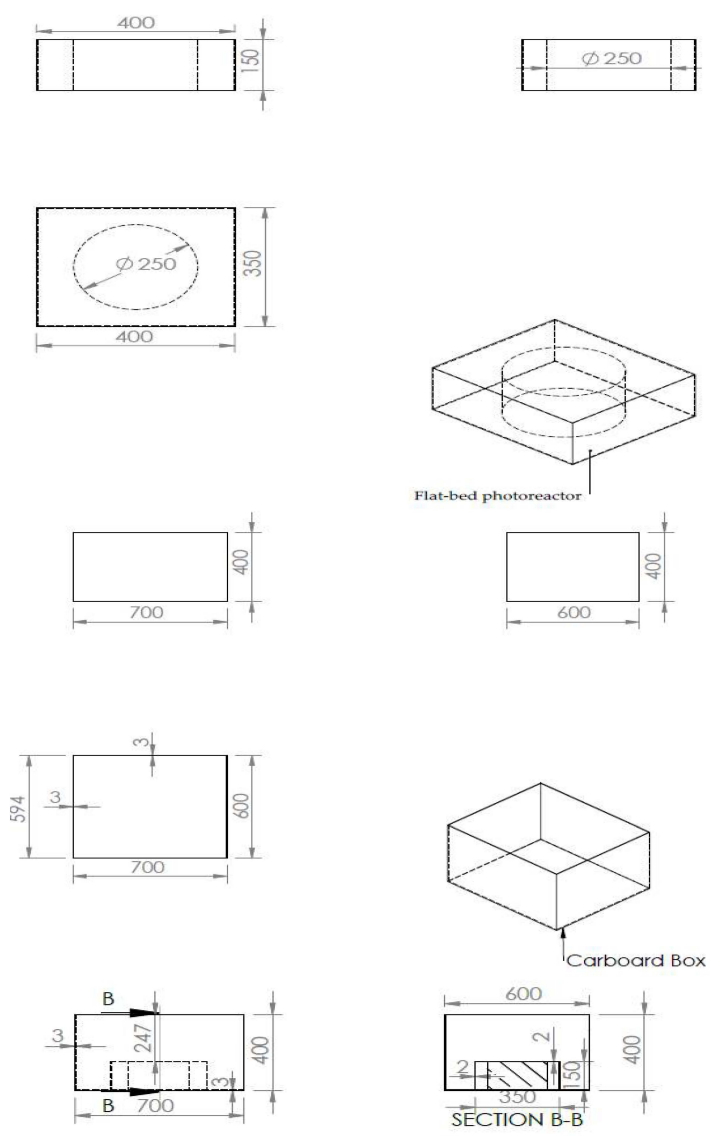


Figure 2. Cont.





**Figure 2.** Different views of the dimensions of the photoreactor.

The introduction of the flat-bed photoreactor was highly efficient by collecting as much photon energy from the sun and destabilizing the  $\pi$ - $\pi$  bonds from the PAHs. The process of photoelectrochemical water splitting, which is also known as the electrolysis process using solar energy to split water molecular ( $\text{H}_2\text{O}$ ) and form  $\text{H}^+$  and  $\text{OH}^-$  should be considered for spontaneous photodegradation of PAHs. These radicals can effectively destroy organic pollutants, however, these radicals were highly reactive when using the flat-bed photoreactor.

## 2.2. Photodegradation Mechanism

There are various species, also known as oxidants or radicals, such as  $\text{O}_2^{\cdot-}$  and  $\text{HO}_2^{\cdot}$ ; however, their oxidation potential is not as high as the hydroxyl ( $\cdot\text{OH}$ ) that can contribute to the photodegradation [49]. These species can be derived naturally under solar irradiation from the water molecule.

During the photodegradation of PAHs, the water molecules are broken down by forming radicals, and these radicals interact with the pollutants by degrading them. According to Li et al. [50],  $\text{h}^+$ ,  $\text{HO}_2^{\cdot}$ ,  $\text{O}_2^{\cdot-}$ , and  $\text{OH}^{\cdot}$  are the most active reagents with regard to degrading organic pollutants. Although they are several scavengers, also known as active reagents, that can degrade the PAHs,  $\text{OH}^{\cdot}$  happens to be widely effective and generable from the water molecule splitting [43]. Its high oxidation potential of  $E(\text{OH}/\text{H}_2\text{O}) = 2.80 \text{ V/SHE}$  makes it better and more effective [51]; although it is the second after fluorine  $E = 3.0 \text{ eV}$  to be commonly responsible for interacting with the PAHs, it can easily be generated from water splitting. Figure 3 demonstrates the mechanism of the splitting of a water molecule triggered by solar irradiation to aid in the photodegradation of PAHs.

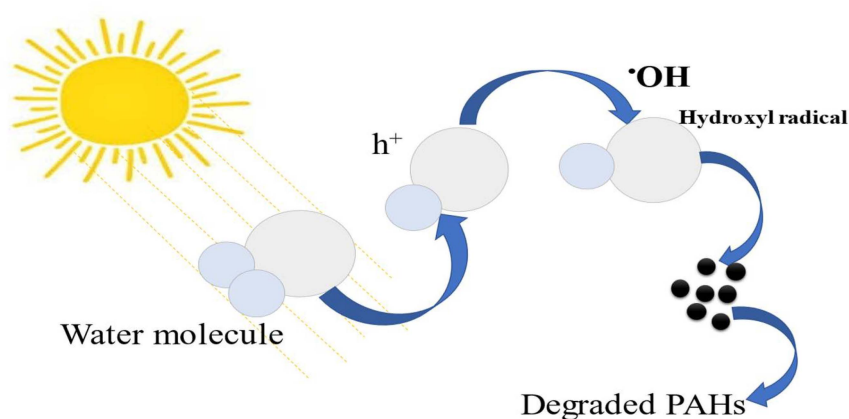


**Figure 3.** The mechanism of the photodegradation of PAHs.

Since organic pollutants have recently gained attention and various techniques have been applied and the application of the photocatalytic has been proven to be highly effective, and eco-friendly; in undertaking complex organic compounds and for spontaneous photodegradation, a presence of light should be acquired [52–54].

A Study by Rani and Karthikeyan [55] was conducted using a self-made photoreactor that was composed of a photocatalytic membrane reactor which was coupled with a

membrane process to assist in the photodegradation of selected PAHs such as PHE, NAP, and ACE under UV light. The photodegradation of PHE, NAP, and ACE at 180 min without the catalyst ( $\text{TiO}_2$ ) and the membrane ultrafiltration (UF) was found to be 8.1, 43.3, and 42.0%, respectively. Afterwards, the addition of a catalyst and membrane resulted in the removal efficiency that varied individually as compared to a sample. A removal efficiency of 83.5, 76.8, and 80.1% individually was found, as compared to the removal efficiency of 85.6, 79.1, and 83.4% for PHE, NAP, and ACE, respectively, that was observed in a sample.

### 3. Results and Discussion

A mass of 116.3 mg with 2 mL of hexane was used to extract and analyse the PAHs in a coal tar using the GC-MS. It was discovered to have a concentration of 2916.47 mg/L of PAHs in total. Table 2 represents the concentration of 16 PAHs found in coal tar. Naphthalene happens to be highly concentrated with 788 mg/L as compared to Indenol[1,2,3-cd] pyrene of 8 mg/L.

**Table 2.** PAHs concentration in a coal tar.

PAHs (Pollutants)	Concentration (mg/L)
NAP	788
ACY	356
ACE	18
FL	327
PHE	632
ANT	245
FLU	395
PYR	266
BaA	91
CHY	126
BbF	75
Blkf	71
BaP	92
DahA	56
IP	8
Bghip	21

Tables 3–5 represent the photodegradation of these 16 PAHs in 20 min, 40 min, and 60 min with and without the flat-bed photoreactor on the acidic mine drainage, alkaline mine drainage, and sewage wastewater.

During the photodegradation of PAHs in various water sources, the water was treated in time periods of 20 min, 40 min, and 60 min, and it was observed that the remaining PAHs in each water source were degraded with a lesser removal efficiency in the shorter time periods. Naphthalene with a lower ring number and lower boiling point, as presented in Table 1, was completely degraded. Acenaphthene, fluorene, dibenzo[a,h]anthracene, pyrene, indenol[1,2,3-cd] pyrene, Benzo[g,h,i]perylene, benzo[b]fluoranthene, and benzo[k]fluoranthene with initial concentrations of 18 mg/L, 395 mg/L, 56 mg/L, 266 mg/L, 8 mg/L, 21 mg/L, 75 mg/L, and 71 mg/L, respectively, in an acidic mine drainage were not degraded. In addition benzo[a]anthracene, chrysene, benzo[b]fluoranthene, benzo[k]fluoranthene, benzo[a]pyrene, dibenzo[a,h]anthracene, indenol[1,2,3-cd] pyrene, and benzo[g,h,i]perylene with initial concentrations of 91 mg/L, 126 mg/L, 75 mg/L, 71 mg/L, 92 mg/L, 56 mg/L, 8 mg/L, and 21 mg/L, in an alkaline mine drainage were also not degraded; moreover, acenaphthene



with an initial concentration of 18 mg/L in sewage wastewater was also not degraded. These PAHs were not degraded at any stage of the photodegradation process; although they were identified in coal tar, they were not dissolved in the water sources left for 8 weeks of dissolution time. The higher molecular weight PAHs happen to have a lower decomposition rate, which was observed in alkaline mine drainage.

**Table 3.** Photodegradation of PAHs in acidic mine drainage (concentrations in mg/L).

PAHs	Initial Concentration	20 min	40 min	60 min	20 min	40 min	60 min
NAP	0.0031	0.0030	0.0017	0.0025	0.0019	0.0016	0.0029
ACY	0.1302	0.1092	0.1267	0.1031	0.1271	0.1098	0.1277
ACE	0	0	0	0	0	0	0
FL	0	0	0	0	0	0	0
PHE	0.0181	0.0083	0.0091	0.0133	0.008	0.0143	0.0176
ANT	18.9847	7.7006	6.7824	6.7014	10.7141	9.5481	8.7359
FLU	0.0020	0.0017	0.0013	0.0013	0.0018	0.0013	0.0016
PYR	0	0	0	0	0	0	0
BaA	0.1114	0.1049	0.1062	0.0517	0.1109	0.1089	0.1093
CHY	0.0012	0	0	0.0007	0.0010	0.0003	0.0009
BbF	0	0	0	0	0	0	0
Blkf	0	0	0	0	0	0	0
BaP	0.0046	0.0042	0.0036	0.0032	0.0042	0.0037	0.0040
DahA	0	0	0	0	0	0	0
IP	0	0	0	0	0	0	0
Bghip	0	0	0	0	0	0	0
PAHs photodegradation	19.2553	7.932	7.031	6.889	10.969	9.788	8.999

**Table 4.** Photodegradation of PAHs in alkaline mine drainage (concentrations in mg/L).

PAHs	Initial Concentration	20 min	40 min	60 min	20 min	40 min	60 min
NAP	0.7615	0.5943	0.5280	0.4212	0.6802	0.6212	0.5212
ACY	0.2596	0.0419	0.0363	0.0139	0.2281	0.1081	0.1281
ACE	0.0020	0.0012	0.0001	0.0001	0	0	0
FL	0.0030	0.0013	0.0012	0.0014	0.0027	0.0019	0.0021
PHE	0.0447	0.0381	0.0216	0.0218	0.0418	0.0359	0.0237
ANT	0.5388	0.2329	0.2194	0.2584	0.5071	0.4112	0.3972
FLU	0.0039	0.0027	0.0019	0.0012	0.0037	0.0028	0.0031
PYR	0.0019	0	0	0	0	0	0
BaA	0	0	0	0	0	0	0
CHY	0	0	0	0	0	0	0
BbF	0	0	0	0	0	0	0
Blkf	0	0	0	0	0	0	0
BaP	0	0	0	0	0	0	0
DahA	0	0	0	0	0	0	0
IP	0	0	0	0	0	0	0
Bghip	0	0	0	0	0	0	0
PAHs photodegradation	1.6154	0.9122	0.8085	0.7180	1.4636	1.1811	1.0754

**Table 5.** Photodegradation of PAHs in sewage wastewater (concentrations in mg/L).

PAHs	Initial Concentration	20 min	40 min	60 min	20 min	40 min	60 min
NAP	0.0069	0.0053	0.0045	0.0047	0.0067	0.0062	0.0053
ACY	0.0489	0.0359	0.0310	0.0224	0.0379	0.0358	0.0302
ACE	0	0	0	0	0	0	0
FL	0.009	0.0067	0.0058	0.0015	0.0011	0.0010	0.0065
PHE	0.0961	0.0177	0.0153	0.0121	0.0821	0.0773	0.0758
ANT	0.1758	0.1502	0.0957	0.1019	0.1508	0.1395	0.1059
FLU	0.1706	0.0197	0.0049	0.0347	0.1607	0.1370	0.1134
PYR	0.1389	0.0149	0.0123	0.0333	0.1297	0.1033	0.0927
BaA	0.1888	0.0158	0.0937	0.1171	0.1251	0.1222	0.1193
CHY	0.1170	0.1002	0.0713	0.0943	0.1078	0.0931	0.1091
BbF	0.2216	0.1506	0.1474	0.1004	0.2004	0.1017	0.1099
Blkf	0.1563	0.0753	0.1132	0.1007	0.1390	0.1031	0.1013
BaP	0.2185	0.1073	0.1175	0.0372	0.2012	0.1109	0.1197
DahA	0.1278	0.0137	0.0109	0.0273	0.1224	0.1006	0.0710
IP	0.0345	0.0063	0.0045	0.0065	0.0217	0.0194	0.0205
Bghip	0.1018	0.0676	0.0507	0.0451	0.0978	0.0501	0.0612
PAHs photodegradation	1.8125	0.7872	0.7787	0.7572	1.5844	1.2002	1.1113

According to Qiao [56], these PAHs emit a specific wavelength, and in this study, these persistent PAHs in each water source were slightly degraded at their specific wavelength.

The photodegradation of the PAHs was conducted at an interval period of 20 min, 40 min and 60 min in acidic mine drainage, alkaline mine drainage and sewage wastewater. It was observed that, as time increases, the removal efficiency of PAHs also increased due to the longer contact time between the photons and the pollutants (PAHs) in the flat-bed photoreactor. The higher removal efficiency occurred in acidic mine drainage as compared to alkaline mine drainage with and without the introduction of the flat-bed photoreactor. The greater the remaining PAHs in each of these water sources, or the closer they are to their initial concentration, the lesser the removal efficiency, and vice versa. In this study, the acidic mine drainage should be given more attention due to its higher PAHs dissolution respective to time. The higher removal efficiency depends on the PAHs' dissolution in the water sources. Besides this, sewage water was the water source where 15 PAHs out of the 16 recognized PAHs were dissolved, and this could be attributed to the water's physiochemical properties, such as total dissolved solids and dissolved organic carbon.

Figure 4A,B represent the photodegradation of the PAHs with (A) a flat-bed photoreactor and (B) without a flat-bed photoreactor, showing better degradation efficiency when the flat-bed photoreactor was used.

Since two sets of experiments were conducted aiming for the photodegradation of PAHs in three water sources, it was discovered that the photodegradation of PAHs in acidic mine drainage was better to dissolve the PAHs rapidly in the leaching process, as reported by Batchamen et al. [11]. The photodegradation was also favoured by both solar irradiation, as shown by Li et al. [50,57], and the time taken for degradation [48]. The photodegradation of PAHs was directly proportional to time and best performed using a flat-bed photoreactor. As shown in Figure 4, the removal efficiency of the PAHs indicates that the flat-bed photoreactor provided a higher removal efficiency. The scavenger ( $\text{OH}^\bullet$ ) was highly reactive in acidic mine drainage as compared to alkaline mine drainage, and this was attributed to the physiochemical properties of the water reported by Batchamen et al. [11].

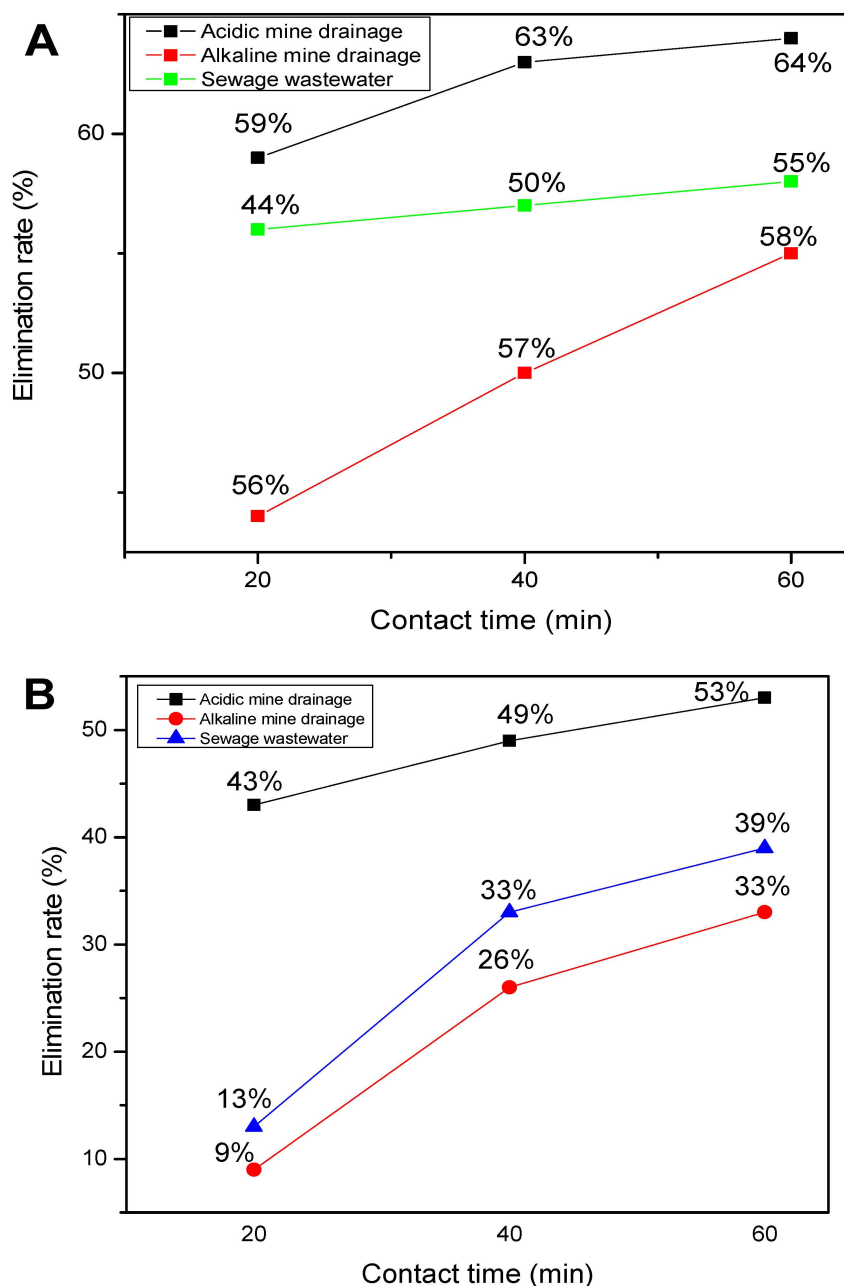


**Figure 4.** Photodegradation of PAHs with (A) a flat-bed photoreactor and (B) without a flat-bed photoreactor.

A comparison of the experiments conducted by Rani et al. [55] on the photodegradation of PAH in an aqueous solution and the results obtained in the present experiment for the AMD, shows that the results of this current study agree with those obtained by Rani et al. [55], which showed that the removal efficiency was higher as compared to the individual PAHs. The introduction of  $\text{TiO}_2$  and UF (UV) in a photoreactor could enhance a 85.6% PHE, 79.1% NAP, and 83.4% ACE removal, whereas with the application of the flat-bed, as was done in the present experiment, almost 100% removal was possible in the three water sources studied.

The photodegradation of PAHs was favoured in the acidic mine drainage, followed by sewage wastewater and alkaline mine drainage. The results reveal that, as time increases, more energy is required from the photon to the chemical energy to destabilize the  $\pi$ - $\pi$  bonds rings in PAHs to anticipate its degradation. The flat-bed photoreactor was able to adapt enough energy due to the materials used and the geometry. The photodegradation after

60 min was not enough to obtain a removal efficiency of 100%, therefore, it is recommended for the photodegradation to go beyond 60 min.

In this study, it was proven that the flat-bed photoreactor was effective, and it was able to decrease both the hydrophobic and immobility of the PAHs by destabilizing them with the help of solar irradiation [53]. However, since the reaction occurred in a system, a few factors, such as the nature of the environment, might influence the reaction, as reported by Matamoros et al. [47]. After the photodegradation, the physiochemical property of these waters, like the total dissolved organic carbon, decreases along with the PAHs pollutant [58]. The application of the flat-bed photoreactor can be recommended as an efficient method for the photodegradation of persistent organic pollutants at any stage and water sources. This flat-bed shows a higher removal efficiency under solar irradiation without any addition of a catalyst; therefore, it can be recommended to be tested with an additional catalyst to enhance the photodegradation of PAHs in various water sources.

#### 4. Conclusions

The photodegradation of PAHs was proven to be spontaneous in the acidic mine drainage, followed by the alkaline mine drainage and sewage wastewater, because of the pH and the total dissolved organic content of these waters, as shown by Batchamen et al. [11]. Solar energy, which is a renewable energy source, was effective in reducing the PAHs in acidic mine drainage, alkaline mine drainage, and sewage wastewater with or without the flat-bed photoreactor. It was also highlighted that as time increased, more contact between the PAHs and the photon took place. The flat-bed photoreactor was effective in producing enough photons to challenge the aromatics rings to degrade the PAHs over time. The removal efficiency was found to be 64%, 55%, and 58% using a flat-bed photoreactor and 53%, 33%, and 39% without the flat-bed photoreactor over time in acidic mine drainage, alkaline drainage, and sewage wastewater, respectively. The hydroxyl species from the water splitting was responsible for taking control of the persistent organic pollutants (PAHs) in the experimental waters. The solar irradiation and the flat-bed photoreactor were highly effective in achieving the aim. The highest removal efficiency was observed in acidic mine drainage, followed by sewage wastewater and alkaline mine drainage.

**Author Contributions:** Conceptualization, J.B.B.M.; Data curation, J.B.B.M.; Formal analysis, J.B.B.M.; Investigation, J.B.B.M.; Methodology, J.B.B.M.; Project administration, J.B.B.M.; Software, J.B.B.M.; Supervision, F.W., E.F.-K. and A.R.A.A.; Validation, J.B.B.M.; Visualization, J.B.B.M.; Writing—original draft, J.B.B.M.; Writing—review & editing, F.W., E.F.-K. and A.R.A.A. All authors have read and agreed to the published version of the manuscript.

**Funding:** This research received no external funding.

**Institutional Review Board Statement:** Not applicable.

**Informed Consent Statement:** Not applicable.

**Data Availability Statement:** Not applicable.

**Acknowledgments:** The authors are thankful to the sponsors: the Water Research Commission (WRC, Project 2974) and the North-West University in South Africa.

**Conflicts of Interest:** The authors declare no conflict of interest.

#### References and Note

1. Rashed, M.N. *Organic Pollutants: Monitoring, Risk and Treatment*; BoD—Books on Demand: Norderstedt, Germany, 2013.
2. Loganath, R.; Mazumder, D. Performance study on organic carbon, total nitrogen, suspended solids removal and biogas production in hybrid UASB reactor treating real slaughterhouse wastewater. *J. Environ. Chem. Eng.* **2018**, *6*, 3474–3484. [[CrossRef](#)]
3. Halicki, W.; Halicki, M. From Domestic Sewage to Potable Water Quality: New Approach in Organic Matter Removal Using Natural Treatment Systems for Wastewater. *Water* **2022**, *14*, 1909. [[CrossRef](#)]
4. Crini, G.; Lichtfouse, E. Advantages and disadvantages of techniques used for wastewater treatment. *Environ. Chem. Lett.* **2019**, *17*, 145–155. [[CrossRef](#)]

5. Abdel-Shafy, H.I.; Mansour, M.S. A review on polycyclic aromatic hydrocarbons: Source, environmental impact, effect on human health and remediation. *Egypt. J. Pet.* **2016**, *25*, 107–123. [\[CrossRef\]](#)
6. Xie, B.; Qin, J.; Sun, H.; Wang, S.; Li, X. Leaching behavior of polycyclic aromatic hydrocarbons (PAHs) from oil-based residues of shale gas drill cuttings. *Environ. Pollut.* **2021**, *288*, 117773. [\[CrossRef\]](#) [\[PubMed\]](#)
7. Mojiri, A.; Zhou, J.L.; Ohashi, A.; Ozaki, N.; Kindaichi, T. Comprehensive review of polycyclic aromatic hydrocarbons in water sources, their effects and treatments. *Sci. Total Environ.* **2019**, *696*, 133971. [\[CrossRef\]](#)
8. Gaurav, G.K.; Mehmood, T.; Kumar, M.; Cheng, L.; Sathishkumar, K.; Kumar, A.; Yadav, D. Review on polycyclic aromatic hydrocarbons (PAHs) migration from wastewater. *J. Contam. Hydrol.* **2021**, *236*, 103715. [\[CrossRef\]](#)
9. Huang, Y.; Li, K.; Liu, H.; Yuan, X.; Li, M.; Xiong, B.; Du, R.; Johnson, D.M.; Xi, Y. Distribution, sources and risk assessment of PAHs in soil from the water level fluctuation zone of Xiangxi Bay, Three Gorges Reservoir. *Environ. Geochem. Health* **2021**, *44*, 2615–2628. [\[CrossRef\]](#)
10. Cai, T.; Ding, Y.; Zhang, Z.; Wang, X.; Wang, T.; Ren, Y.; Dong, Y. Effects of total organic carbon content and leaching water volume on migration behavior of polycyclic aromatic hydrocarbons in soils by column leaching tests. *Environ. Pollut.* **2019**, *254*, 112981. [\[CrossRef\]](#)
11. Batchamen Mougno, J.B.; Waanders, F.; Fosso-Kankeu, E.; Al Alili, A.R. Leaching of Polycyclic Aromatic Hydrocarbons from the Coal Tar in Sewage Wastewater, Acidic and Alkaline Mine Drainage. *Int. J. Environ. Res. Public Health* **2022**, *19*, 4791. [\[CrossRef\]](#)
12. Singh, S.; Haritash, A. Polycyclic aromatic hydrocarbons: Soil pollution and remediation. *Int. J. Environ. Sci. Technol.* **2019**, *16*, 6489–6512.
13. Adeniji, A.O.; Okoh, O.O.; Okoh, A.I. Analytical methods for polycyclic aromatic hydrocarbons and their global trend of distribution in water and sediment: A review. *Recent Insights Pet. Sci. Eng.* **2018**, *10*. [\[CrossRef\]](#)
14. Smol, M.; Włoka, D.; Włodarczyk-Makuła, M. Influence of integrated membrane treatment on the phytotoxicity of wastewater from the coke industry. *Water Air Soil Pollut.* **2018**, *229*, 154. [\[CrossRef\]](#)
15. Bolden, A.L.; Rochester, J.R.; Schultz, K.; Kwiatkowski, C.F. Polycyclic aromatic hydrocarbons and female reproductive health: A scoping review. *Reprod. Toxicol.* **2017**, *73*, 61–74. [\[CrossRef\]](#) [\[PubMed\]](#)
16. Davie-Martin, C.L.; Stratton, K.G.; Teeguarden, J.G.; Waters, K.M.; Simonich, S.L.M. Implications of bioremediation of polycyclic aromatic hydrocarbon-contaminated soils for human health and cancer risk. *Environ. Sci. Technol.* **2017**, *51*, 9458–9468. [\[CrossRef\]](#) [\[PubMed\]](#)
17. Alghamdi, M.A.; Hassan, S.K.; Al Sharif, M.Y.; Khoder, M.I.; Harrison, R.M. On the nature of polycyclic aromatic hydrocarbons associated with sporting walkways dust: Concentrations, sources and relative health risk. *Sci. Total Environ.* **2021**, *781*, 146540. [\[CrossRef\]](#) [\[PubMed\]](#)
18. Shamsedini, N.; Dehghani, M.; Samaei, M.; Azhdarpoor, A.; Hoseini, M.; Fararouei, M.; Bahrany, S.; Roosta, S. Health risk assessment of polycyclic aromatic hydrocarbons in individuals living near restaurants: A cross-sectional study in Shiraz, Iran. *Sci. Rep.* **2022**, *12*, 8254. [\[CrossRef\]](#) [\[PubMed\]](#)
19. Li, W.; Park, R.; Alexandrou, N.; Dryfhout-Clark, H.; Brice, K.; Hung, H. Multi-year analyses reveal different trends, sources, and implications for source-related human health risks of atmospheric polycyclic aromatic hydrocarbons in the Canadian Great Lakes Basin. *Environ. Sci. Technol.* **2021**, *55*, 2254–2264. [\[CrossRef\]](#)
20. Gopinath, A.; Divyapriya, G.; Srivastava, V.; Laiju, A.; Nidheesh, P.; Kumar, M.S. Conversion of sewage sludge into biochar: A potential resource in water and wastewater treatment. *Environ. Res.* **2021**, *194*, 110656. [\[CrossRef\]](#)
21. Bora, A.P.; Gupta, D.P.; Durbha, K.S. Sewage sludge to bio-fuel: A review on the sustainable approach of transforming sewage waste to alternative fuel. *Fuel* **2020**, *259*, 116262. [\[CrossRef\]](#)
22. Mondala, A.H.; Hernandez, R.; French, T.; McFarland, L.; Santo Domingo, J.W.; Meckes, M.; Ryu, H.; Iker, B. Enhanced lipid and biodiesel production from glucose-fed activated sludge: Kinetics and microbial community analysis. *AIChE J.* **2012**, *58*, 1279–1290. [\[CrossRef\]](#)
23. Agoro, M.A.; Adeniji, A.O.; Adefisoye, M.A.; Okoh, O.O. Heavy metals in wastewater and sewage sludge from selected municipal treatment plants in Eastern Cape Province, South Africa. *Water* **2020**, *12*, 2746. [\[CrossRef\]](#)
24. Titilawo, Y.; Adeniji, A.; Adeniyi, M.; Okoh, A. Determination of levels of some metal contaminants in the freshwater environments of Osun State, Southwest Nigeria: A risk assessment approach to predict health threat. *Chemosphere* **2018**, *211*, 834–843. [\[CrossRef\]](#)
25. Nyamukamba, P.; Moloto, M.J.; Tavengwa, N.; Ejidike, I.P. Evaluating physicochemical parameters, heavy metals, and antibiotics in the influents and final effluents of South African wastewater treatment plants. *Pol. J. Environ. Stud.* **2019**, *28*, 1305–1312. [\[CrossRef\]](#)
26. Grobelak, A.; Grosser, A.; Kacprzak, M.; Kamizela, T. Sewage sludge processing and management in small and medium-sized municipal wastewater treatment plant-new technical solution. *J. Environ. Manag.* **2019**, *234*, 90–96. [\[CrossRef\]](#) [\[PubMed\]](#)
27. Pozo-Antonio, S.; Puente-Luna, I.; Lagüela-López, S.; Veiga-Ríos, M. Techniques to correct and prevent acid mine drainage: A review. *Dyna* **2014**, *81*, 73–80. [\[CrossRef\]](#)
28. Dold, B. Evolution of acid mine drainage formation in sulphidic mine tailings. *Minerals* **2014**, *4*, 621–641. [\[CrossRef\]](#)
29. Simate, G.S.; Ndlovu, S. Acid mine drainage: Challenges and opportunities. *J. Environ. Chem. Eng.* **2014**, *2*, 1785–1803. [\[CrossRef\]](#)
30. Rodríguez-Galán, M.; Baena-Moreno, F.M.; Vázquez, S.; Arroyo-Torrvalvo, F.; Vilches, L.F.; Zhang, Z. Remediation of acid mine drainage. *Environ. Chem. Lett.* **2019**, *17*, 1529–1538. [\[CrossRef\]](#)

31. Kaur, G.; Couperthwaite, S.J.; Hatton-Jones, B.W.; Millar, G.J. Alternative neutralisation materials for acid mine drainage treatment. *J. Water Process Eng.* **2018**, *22*, 46–58. [\[CrossRef\]](#)
32. Skousen, J.; Zipper, C.E.; Rose, A.; Ziemkiewicz, P.F.; Nairn, R.; McDonald, L.M.; Kleinmann, R.L. Review of passive systems for acid mine drainage treatment. *Mine Water Environ.* **2017**, *36*, 133–153. [\[CrossRef\]](#)
33. Zipper, C.E.; Skousen, J.G.; Jage, C.R. Passive treatment of acid-mine drainage. 2018.
34. Vidal, R.; Moraes, J. Removal of organic pollutants from wastewater using chitosan: A literature review. *Int. J. Environ. Sci. Technol.* **2019**, *16*, 1741–1754. [\[CrossRef\]](#)
35. Nisticò, R.; Cesano, F.; Franzoso, F.; Magnacca, G.; Scarano, D.; Funes, I.G.; Carlos, L.; Parolo, M.E. From biowaste to magnet-responsive materials for water remediation from polycyclic aromatic hydrocarbons. *Chemosphere* **2018**, *202*, 686–693. [\[CrossRef\]](#) [\[PubMed\]](#)
36. Rashed, M.N. Adsorption technique for the removal of organic pollutants from water and wastewater. *Org. Pollut. Monit. Risk Treat.* **2013**, *7*, 167–194.
37. Roy, A.; Murthy, H.A.; Ahmed, H.M.; Islam, M.N.; Prasad, R. Phytogenic synthesis of metal/metal oxide nanoparticles for degradation of dyes. *J. Renew. Mater.* **2022**, *10*, 1911. [\[CrossRef\]](#)
38. Varjani, S.J. Microbial degradation of petroleum hydrocarbons. *Bioresour. Technol.* **2017**, *223*, 277–286. [\[CrossRef\]](#)
39. Akinpelu, A.A.; Ali, M.E.; Johan, M.R.; Saidur, R.; Qurban, M.A.; Saleh, T.A. Polycyclic aromatic hydrocarbons extraction and removal from wastewater by carbon nanotubes: A review of the current technologies, challenges and prospects. *Process Saf. Environ. Prot.* **2019**, *122*, 68–82. [\[CrossRef\]](#)
40. Patel, A.B.; Shaikh, S.; Jain, K.R.; Desai, C.; Madamwar, D. Polycyclic aromatic hydrocarbons: Sources, toxicity and remediation approaches. *Front. Microbiol.* **2020**, *11*, 2675. [\[CrossRef\]](#)
41. Taghipour, F. UV-LED Radiation Photoreactor. U.S. Patent 20180201521A1, 5 May 2020.
42. Sundar, K.P.; Kanmani, S. Progression of Photocatalytic reactors and it's comparison: A Review. *Chem. Eng. Res. Des.* **2020**, *154*, 135–150. [\[CrossRef\]](#)
43. Purcar, V.; Rădițoiu, V.; Rădițoiu, A.; Raduly, F.M.; Manea, R.; Frone, A.; Anastasescu, M.; Ispas, G.C.; Căprărescu, S. Bilayer coatings based on silica materials and iron (III) phthalocyanine–Sensitized TiO<sub>2</sub> photocatalyst. *Mater. Res. Bull.* **2021**, *138*, 111222. [\[CrossRef\]](#)
44. Bandala, E.R.; Arancibia-Bulnes, C.A.; Orozco, S.L.; Estrada, C.A. Solar photoreactors comparison based on oxalic acid photocatalytic degradation. *Sol. Energy* **2004**, *77*, 503–512. [\[CrossRef\]](#)
45. Chen, M.; He, Y.; Zhu, J.; Wen, D. Investigating the collector efficiency of silver nanofluids based direct absorption solar collectors. *Appl. Energy* **2016**, *181*, 65–74. [\[CrossRef\]](#)
46. Tzivanidis, C.; Bellos, E.; Korres, D.; Antonopoulos, K.; Mitsopoulos, G. Thermal and optical efficiency investigation of a parabolic trough collector. *Case Stud. Therm. Eng.* **2015**, *6*, 226–237. [\[CrossRef\]](#)
47. Matamoros, V.; Gutiérrez, R.; Ferrer, I.; García, J.; Bayona, J.M. Capability of microalgae-based wastewater treatment systems to remove emerging organic contaminants: A pilot-scale study. *J. Hazard. Mater.* **2015**, *288*, 34–42. [\[CrossRef\]](#) [\[PubMed\]](#)
48. Gu, J.; Dong, D.; Kong, L.; Zheng, Y.; Li, X. Photocatalytic degradation of phenanthrene on soil surfaces in the presence of nanometer anatase TiO<sub>2</sub> under UV-light. *J. Environ. Sci.* **2012**, *24*, 2122–2126. [\[CrossRef\]](#)
49. Chiu, Y.-H.; Chang, T.-F.M.; Chen, C.-Y.; Sone, M.; Hsu, Y.-J. Mechanistic insights into photodegradation of organic dyes using heterostructure photocatalysts. *Catalysts* **2019**, *9*, 430. [\[CrossRef\]](#)
50. Li, P.; Kim, S.; Jin, J.; Do, H.C.; Park, J.H. Efficient photodegradation of volatile organic compounds by iron-based metal-organic frameworks with high adsorption capacity. *Appl. Catal. B Environ.* **2020**, *263*, 118284. [\[CrossRef\]](#)
51. Sudhaik, A.; Raizada, P.; Shandilya, P.; Jeong, D.-Y.; Lim, J.-H.; Singh, P. Review on fabrication of graphitic carbon nitride based efficient nanocomposites for photodegradation of aqueous phase organic pollutants. *J. Ind. Eng. Chem.* **2018**, *67*, 28–51. [\[CrossRef\]](#)
52. Wang, C.; Li, Y.; Tan, H.; Zhang, A.; Xie, Y.; Wu, B.; Xu, H. A novel microbe consortium, nano-visible light photocatalyst and microcapsule system to degrade PAHs. *Chem. Eng. J.* **2019**, *359*, 1065–1074. [\[CrossRef\]](#)
53. Eker, G.; Hatipoglu, M. Effect of UV wavelength, temperature and photocatalyst on the removal of PAHs from industrial soil with photodegradation applications. *Environ. Technol.* **2018**, *40*, 3793–3803. [\[CrossRef\]](#)
54. Sliem, M.A.; Salim, A.Y.; Mohamed, G.G. Photocatalytic degradation of anthracene in aqueous dispersion of metal oxides nanoparticles: Effect of different parameters. *J. Photochem. Photobiol. A Chem.* **2019**, *371*, 327–335. [\[CrossRef\]](#)
55. Rani, C.N.; Karthikeyan, S. Synergic effects on degradation of a mixture of polycyclic aromatic hydrocarbons in a UV slurry photocatalytic membrane reactor and its cost estimation. *Chem. Eng. Processing-Process Intensif.* **2021**, *159*, 108179. [\[CrossRef\]](#)
56. Qiao, Y. Preparation, Characterization, and Evaluation of Photocatalytic Properties of a Novel NaNbO<sub>3</sub>/Bi<sub>2</sub>WO<sub>6</sub> Heterostructure Photocatalyst for Water Treatment. Ph.D. Thesis, University of Ottawa, Ottawa, ON, Canada, 2018.
57. Nagaraju, P.; Puttaiah, S.H.; Wantala, K.; Shahmoradi, B. Preparation of modified ZnO nanoparticles for photocatalytic degradation of chlorobenzene. *Appl. Water Sci.* **2020**, *10*, 137. [\[CrossRef\]](#)
58. Gupta, A.; Pandey, O. Visible irradiation induced photodegradation by NbC/C nanocomposite derived from smoked cigarette litter (filters). *Sol. Energy* **2018**, *163*, 167–176. [\[CrossRef\]](#)